International Conference Organised by
IBPSA-Nordic, 13th–14th October 2020,
OsloMet

BuildSIM-Nordic 2020

Selected papers

SINTEF   IBPSA   OsloMet

SINTEF Proceedings

Editors:
Laurent Georges, Matthias Haase, Vojislav Novakovic and Peter G. Schild

BuildSIM-Nordic 2020

Selected papers

International Conference Organised by IBPSA-Nordic,
13th–14th October 2020, OsloMet

Keywords:
Building acoustics, Building Information Modelling (BIM), Building physics, CFD and air flow, Commissioning and control, Daylighting and lighting, Developments in simulation, Education in building performance simulation, Energy storage, Heating, Ventilation and Air Conditioning (HVAC), Human behavior in simulation, Indoor Environmental Quality (IEQ), New software developments, Optimization, Simulation at urban scale, Simulation to support regulations, Simulation vs reality, Solar energy systems, Validation, calibration and uncertainty, Weather data & Climate adaptation, Fenestration (windows & shading), Zero Energy Buildings (ZEB), Emissions and Life Cycle Analysis

Cover illustration: IBPSA-logo

A coordinated control to improve energy performance for a building cluster with energy storage, EVs, and energy sharing

Pei Huang[1*], Xingxing Zhang[1], Chris Bales[1], Tomas Persson[1]

[1]Energy Technology, Dalarna University, Borlänge, 79188, Sweden

*corresponding author: phn@du.se

Abstract

Existing studies have developed some advanced controls for energy storage system charging/discharging in a building cluster (enabling PV power sharing among different buildings), which can effectively improve the aggregated performances. However, in the existing controls, the flexible demand shifting ability of electric vehicles (EVs) are rarely considered, leading to limited performance improvements at building cluster level. Thus, this study proposes a coordinated control of building cluster with both energy sharing and the EV charging considered, with the purpose of improving the cluster-level performance. The simulation results show that in a typical summer week in Sweden, the developed control can increase the cluster-level daily renewable self-consumption by 40% and meanwhile reduce the electricity bills by as much as 20% compared with conventional controls for a summer week in Ludvika, Sweden.

1. Introduction

The integration of distributed energy systems has promoted the transformation of buildings' role from energy consumers to energy prosumers, i.e. energy consumers who produce energy for their own consumption using distributed energy technologies (Huang, Copertaro et al. 2020). The transformation of buildings' role into energy prosumers provides opportunities for collaborations among buildings to improve the overall cluster-level performances. When multiple building prosumers are in a building cluster, they can share their excessive renewables with others in shortage (Fan, Huang et al. 2018). Such energy sharing can help improve the building-cluster-level renewable self-consumption rates and thus reduce the grid power usage (due to an increased share of renewable energy utilization). A study conducted by Luthander *et al.* (2016) shows that that even a simple energy sharing (i.e. aggregate electricity demand and supply) among 21 houses in Sweden can easily improve the PV power self-consumption by over 15%. While when there is shared energy storage, the improvement in PV power self-consumption can even reach 29%.

To achieve energy sharing among buildings, existing studies have developed a number of advanced controls. For example, Odonkor *et al.* (2015) proposed a control method of zero energy buildings (ZEBs) using genetic algorithm and Pareto decision making based on an adaptive bi-level decision model (with a facilitator agent at cluster level and local systems at single NZEB level) (Odonkor and Lewis, 2015). Fan *et al.* (2018) proposed a collaborative demand response control of zero energy buildings for enhancing the building-cluster-level performances. In their method, the control of each building was conducted in sequence, and the optimization of one building's operation was based on the previously optimized buildings' operation (Fan *et al.,* 2018). Prasad and Dusparic developed a Deep Reinforcement Learning based method for ZEB community (Prasad and Dusparic 2019). The abovementioned controls optimize the building cluster performance in a bottom-up way, and they merely perform very limited collaborations among buildings. With the purpose of maximizing the energy sharing within a building cluster, researchers have developed controls that directly use the building-cluster-level performances as the optimization targets. For instance, Huang et al. developed a top-down control for a cluster of building prosumers equipped with electrical energy storage system (Huang, Wu et al. 2018). In their study, the optimal performances that can be achieved are first searched by using an advanced searching algorithm. Then the optimal performances at the top-level are divided into separate goals for each individual building at the bottom-level. Similarly, in a three-step demand response control algorithm is developed considering the dynamic pricing. Taking into account of the demand prediction uncertainty, in a robust collaborative control is developed.

These existing controls can effectively improve the performances at building cluster level. However, electric vehicles (EV), which also play an important role in the building cluster scale energy systems, are usually considered as non-scheduled electrical loads (such as lighting) and their flexible demand shifting ability is rarely used (Taşcıkaraoğlu, 2018; Huang, *et al.*, 2019). As a result, the flexible demand shifting ability of EVs are rarely considered together with the building control, leading to limited performance improvements at building cluster level (Barone *et al.*, 2019; Dallinger *et al.*, 2013). For instance, in practice the EV charging will start once they are plugged into charging stations. However, in such charging period the renewable generation may be insufficient to cover the EV charging load, leading to grid electricity imports. On the other hand, when there is surplus renewable generation, the EVs cannot be used as electricity storage if they have already been fully charged,

leading to the surplus renewable energy exports. As a result, the overall building-cluster-level performance is not fully optimized.
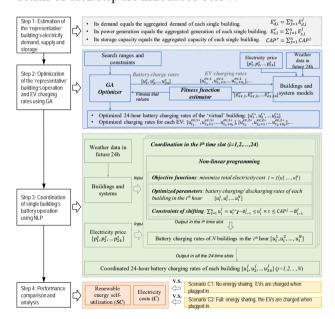
By properly scheduling the EV charging loads, the batteries in EVs can be used as flexible energy storage to help regulate the electricity demands in the power grid. Existing studies have also developed some advanced controls for EVs. For instance, Geth et al. developed a coordinated charging control for a number of EVs (Geth, Willekens et al. 2010). In their control, a vehicle owner first indicates the point in time when the batteries should be fully charged. Then, the aggregator collects this information and calculates when each EV can start charging, based on two rules: (i) charging is most economically when the total demand (including the residential, industrial and EV consumption) is low, and (ii) the EVs can be charged during working hour in the working places. Similarly, Usman et al. proposed an automated coordinated control of EV fleets, which can plan the charging strategy at the cheaper moments while keeping the vehicle charged enough to complete its scheduled trips (Usman, Knapen et al. 2016). Their control uses a grid agent to grant tokens to the EVs in idle state based on the grid electricity prices. By shifting charging loads to low electricity price period (usually with low aggregated electricity demands in the power grid), this control can effectively increase the match between the available power and the consumed power. The abovementioned studies can effectively improve the economic performances of EV or EV fleets. However, these studies typically consider EVs as a separate role in the urban energy system and thus neglect their integration with the building controls.

To sum up, the existing studies have developed some advanced building side controls, which enables renewable energy sharing and aims at optimizing building-cluster-level performance via regulating the energy storage charging/discharging. However, the flexible demand shifting capability of EVs is not considered in the cluster-level controls. Therefore, this study proposes a coordinated control of building cluster with both energy sharing and the EV charging considered, with the purpose of improving the cluster-level performance by taking advantage of energy sharing and storage capability of electricity batteries in both buildings and EVs.

2. Methodology

This section introduces the developed coordinated control. Fig. 1 presents the flowchart of the developed control optimization method. The aim of the coordinated control is to coordinate the operation of energy storage (installed in each single building) and the EVs, to achieve the optimal cluster-level performances. The coordinated control consists of four steps. In Step 1, all the buildings in the building group are considered as a 'representative' building, and the electrical demand, renewable energy generation and load shifting capacity of the 'representative' building are predicted, i.e. its electrical

demand/renewable generation/demand shifting capacity equals the aggregated demand/ generation/capacity of all buildings inside the cluster. In Step 2, the operation of the 'representative' building and the EV charging rates are optimized using genetic algorithm (GA). The performance of the 'representative' building, obtained by simultaneous optimization of the building and EV operation, is considered to be the best performances that the building group can achieve (Shen, Li et al. 2016). In Step 3, the operation of each single building inside the building group is coordinated using non-linear programming (NLP) based on the 'representative' building's operation obtained from Step 2. In Step 4, the performances of the proposed coordinated control are compared with two existing controls, including a conventional individual control (Scenario 1 (Shen, Li et al. 2016)), which does not enable renewable sharing and charge the EVs immediately after being parked, and an existing coordinated control (Scenario 2 (Gao and Sun 2016)), which enables full renewable energy sharing but also charges the EVs immediately after being parked. The details of each step are introduced below.

Figure 1 Flowchart of the coordinated control

Step 1: *Estimation of the 'representative' building's demand and storage*

In this step, all the buildings inside the cluster are considered as a 'virtual' building. Its hourly electricity demand ($E_{d,i}^r$ (kW·h)) equals the aggregated hourly electricity demand (including the household electricity, and electricity for heating or heat pumps) of each single building ($E_{d,i}^j$ (kW·h)) (i indicates time with a unit of hour), its hourly renewable generation ($E_{s,i}^r$ (kW·h)) equals the aggregated hourly renewable generation of each single building ($E_{s,i}^j$ (kW·h)) and its load shifting capacity (CAP^r (kW·h), i.e. battery capacity) is the aggregated load shifting capacity of each single building (CAP^j (kW·h)).

Step 2: *Optimization of the 'representative' building's operation using GA*

The GA algorithm searches the optimal charging/ discharging rates of both the battery and EVs that can minimize the electricity costs of the 'representative' building. For example, the EVs can be scheduled to be charged in periods with sufficient renewable generations while not charged in periods with insufficient generations. In the GA simulation, the inputs mainly include the battery charging/discharging rates (to be optimized), the EV charging rates (to be optimized), the EV parking periods, the future 24-hour weather data, building parameters, and battery parameters. The EVs are different from the building integrated electricity storage system, as they are not constantly connected into the buildings. This study uses four parameters to characterize an EV (e.g. the kth EV): arrival time to the charging port (t^k), parking periods in the charging port (n^k), initial state of charge (SOC_0^k), and the required state of charge when the car departs from the charging port (SOC_1^k). These parameters are considered known and will be used as inputs in the optimization.

In each generation of GA, trials of 24-hour thermal storage hourly charging/discharging rates (i.e., $[u_1^v, u_2^v, ... u_{24}^v]$ kW) and charging rates of each EV (i.e. $[u_{t_k}^{ev,k}, u_{t_k+1}^{ev,k}, ... u_{t_k+n_k}^{ev,k}]$ kW) are generated by the GA optimizer. The representative building's hourly power demand ($E_{d,i}^r$ kW) and hourly renewable power generation ($E_{r,i}^r$ kW) in the future 24 hours is then predicted using the building and system models. The charging/discharging rates of the electrical battery should meet the following two constraints:

(i) The battery charging amount could not exceed the remaining battery storage capacity.

(ii) The battery discharging amount could not exceed the stored electricity in the battery. These two constraints are expressed by Eqn. (4) (Lu, Wang et al. 2015),

$$0 \leq \emptyset_0^r + (u_1^r + u_2^r + \cdots + u_i^r) \times \tau \leq CAP^r \quad \text{where } i=1,2,...,24 \quad (1)$$

where $\emptyset_0^v$ (kW·h) is the amount of electricity energy initially stored in the electrical energy storage system, τ is the duration of battery charging/discharging (i.e., 1 hour in this study).

Similarly, the charging rates of the kth EV should meet these two constraints, as expressed by Eqn. (2). $SOC_{0,k}$ is the initial state of charge when the kth EV arrives at the charging port. CAP_k^{ev} (kW·h) is the capacity of the kth EV battery. t_k is the arrival time of the kth EV at the charging port, and n_k is the parking duration.

$$0 \leq SOC_{0,k} \times CAP_k^{ev} + (u_{t_k}^{ev,k} + u_{t_k+1}^{ev,k} + u_{t_k+i}^{ev,k}) \times \tau \leq CAP_k^{ev}$$
$$\text{where } i=1,2,...,n_k \quad (2)$$

In addition, the EV battery should be charged to a user-specified level ($SOC_{1,k}$) before they depart the charging port. This constraint is expressed by Eqn. (3). When $SOC_{1,k}$ equals 1, it represents the EV users require the EV battery to be fully charged before they depart the charging port.

$$SOC_{0,k} \times CAP_k^{ev} + (u_{t_k}^{ev,k} + u_{t_k+1}^{ev,k} + \cdots + u_{t_k+n_k}^{ev,k}) \times \tau \geq SOC_{1,k} \times CAP_k^{ev} \quad (3)$$

This study considers the strategy to minimize daily electricity cost of the building group. Following this control goal, a fitness function is determined, as expressed by Eqn. (4) (Salom, Widén et al. 2011).

$$J_{grid} = \min(Cost) \quad (4)$$

$$Cost = \sum_{i=1}^{24} E_{ex,i}^r \times \tau \times \chi_i, \begin{cases} \chi_i = \chi_{buy}, if \ E_{ex,i}^r > 0 \\ \chi_i = \chi_{sell}, if \ E_{ex,i}^r \leq 0 \end{cases} \quad (5)$$

where χ_i (kr/(kW·h)) is the electricity price in the ith time slot. χ_{buy} (kr/(kW·h)) is the price of purchasing electricity from the power grid, and χ_{sell} (kr/(kW·h)) is the feed-in-tariff. The outputs of the GA search are the 'representative' building's battery charging/discharging rates ($[u_1^{r*}, u_2^{r*}, ... u_3^{r*}]$ kW) in the next 24 hours and the charging rates of each individual EV ($[u_{t_1}^{ev,1*}, u_{t_k+1}^{ev,k*}, ... , u_{t_k+n_k}^{ev,k*}]$, ... kW). The optimized battery charging/ discharging rates of the 'representative' building are used in Step 3.

Step 3: *Coordination of single building's operation using NLP*

In this step, the single building's battery charging/discharging rates (i.e. u_i^j is the jth building in the ith hour) are coordinated using NLP based on the 'representative' building's operation (Zhao, Lu et al. 2015). The NLP is conducted in each hour and will be repeated 24 times for obtaining the building's daily operation. The fitness function of the NLP is expressed by Eqns. (6) and (7), which aims at minimizing the electricity costs of the building group.

$$J_{NLP} = \min(Cost_{all,i}) \quad (6)$$

$$Cost_{all,i} = \sum_{j=1}^{n} (E_{d,i}^j \times \chi_i)^2 \quad (7)$$

In order to reduce the uneven allocation of the battery charging/discharging rates (otherwise only a few buildings take benefits from the demand response), the square of each building's operational cost is used in the fitness function. $E_{d,i}^j$ (kW·h) is the energy demand of the jth building in the ith hour after applying the u_i^j (kW) amount of battery charging/discharging, which is calculated by the models presented in Section 3. χ_i (HKD/(kW·h)) is the electricity price in the ith hour. In the ith hour, the optimized parameters in the NLP are the hourly battery charging/discharging rates of all the buildings inside the building group, i.e., $[u_i^1, u_i^2, ... , u_i^N]$ (kW), where N indicates the number of buildings in the building group. The battery charging/discharging rates in each hour should follow the constraints below.

(i) The sum of battery charging/discharging rates of each building (u_i^j (kW)) should equal the battery charging/discharging of the 'representative' building (u_i^{r*} (kW)) (obtained from Step 2).

$$\sum_{j=1}^{N} u_i^j = u_i^{r*} \quad (8)$$

(ii) For each single building, the electricity charging amount must be smaller than the remaining storage capacity of the battery, and the electricity discharging amount must be smaller than the amount of electricity stored in the battery. There are 2N inequality constraints for N buildings.

$$-\emptyset_{i-1}^j \leq u_i^j \times \tau \leq CAP^j - \emptyset_{i-1}^j \quad \text{(j=1,2,...N, respectively)} \quad (9)$$

where τ is the charging duration (i.e., 1 hour), CAP^j (kWh) is the battery capacity of the jth building, $\emptyset_{i-1}^j$ (kW·h) is the electricity energy stored in the jth building's battery. $\emptyset_{i-1}^j$ (kW·h) is calculated by Eqn. (10).

$$\emptyset_{i-1}^j = (u_1^j + u_2^j + \cdots + u_{i-1}^j) \times \tau \quad (10)$$

***Step 4:** Performance comparison and analysis*

In this step, the performances of the proposed coordinated control are compared with two existing controls in aspects of renewable energy self-consumption improvements and economic cost savings. The two existing controls include a conventional individual control (Scenario 1 (Shen, Li et al. 2016) (Gao and Sun 2016)), which does not enable renewable sharing and charge the EVs immediately after connecting them, and an existing coordinated control (Scenario 2 (Huang, Wu et al. 2018)), which enables full renewable energy sharing in the building cluster but charges the EVs immediately after connecting them. In both the two comparative studies, the EVs demand are first computed and then added to the building electricity demand, which will then be used as inputs for battery charging/discharging controls. In Scenario 1 (i.e. an existing individual control) (Shen *et al.* 2016), GA was used for searching the optimal battery charging/discharging rates in each building, which is similar to the control optimization of the 'representative' building (see Step 2 in Fig. 2 without EV related variables). After obtaining the individual buildings' optimal operation, their electrical demands were aggregated for evaluating the building-cluster-level performances. In Scenario 2 (i.e. an existing coordinated control) (Gao and Sun, 2016), the battery charging/discharging rates of all the three buildings are optimized simultaneously using GA, and the minimization of the building-cluster-level performance was used as the fitness function.

Table 1 Configuration of the three scenarios

Scenario	EV control?	Energy sharing?
1	Charged immediately when plugged in	No
2	Charged immediately when plugged in	Full sharing
3	Charged at any time when parked	Full sharing

3. Buildings and system modelling

This section introduces the building information and system modelling. Each building is installed with a renewable energy system (i.e., PV panels), an electricity storage system (i.e., battery), as well as an EV.

3.1 Building modelling

This study considered a real building cluster located in Ludvika, Dalarna region, Sweden. This building cluster consists of three separate buildings, as shown in Fig. 2. These buildings will be improved by a series of renovation plans including installation of PV, battery storage, direct current (DC) micro grid, and EV charging station. It is assumed the heating is provided by district heating system. So, the PV panels will only need to provide power supply to the domestic electricity demand (e.g. lighting, TVs, dish wash).

Figure 2 Bird view of the case building cluster located in Ludvika, Sweden

3.2 Renewable energy system modeling

The power generation from the PV panel P_{PV} (kW) is calculated by Eqn. (14) (Klein *et al.*, 2004),

$$P_{PV} = \tau \times I_{AM} \times I_T \times \eta \times CAP_{PV} \quad (11)$$

where τ is the transmittance-absorptance product of the PV cover for solar radiation at a normal incidence angle, ranging from 0 to 1; I_{AM} is the combined incidence angle modifier for the PV cover material, ranging from 0 to 1; I_T (W/m^2) is the total amount of solar radiation incident on the PV collect surface; η is the overall efficiency of the PV array; CAP_{PV} (m^2) is the PV surface area. The local weather data in Ludivika was used as inputs with a time resolution of 1 hour.

3.3 Electrical battery and EV battery modeling

This study used simplified electrical battery and EV battery models. The electricity stored in the battery is calculated using a simplified model, as expressed by Eqns. (4) and (5). It is estimated from the hourly charging rates (Sun, Huang et al. 2018). This study considers three EVs. Table 2 summarizes the capacity, maximum charging rates as well as the parking periods of each EV. EV 1, EV 2 and EV 3 are assumed to be charged in Building A, B and C, respectively. To consider the various EV usage, these three EVs are assumed to have different parking periods. EV 1 is assumed to be owned by a resident living in the building, and thus it is parked at night from 18:00 to 07:00 in the next day. EV 2 and EV 3 are assumed to be owned by some working staff in the building estate, and they are parked during daytime (i.e. one from 08:00~16:00 and the other from 09:00~17:00). The EV battery capacity and maximum charging rates are referred from the available EV models in the market in (Ustun, Zayegh et al. 2013).

Table 2 Capacity, charging limits and parking periods of the three different EVs, data obtained from (Ustun, Zayegh et al. 2013)

ID	Battery capacity (kW·h)	Maximum charging rates (kW)	Parking period
EV 1	22	4	18:00~07:00
EV 2	27	5	08:00~16:00
EV 3	53	10	09:00~17:00

In all the three scenarios, the EVs are required to be fully charged before they leave the charging station (Note that the time of departure is considered as a known parameter set by the EV owners). When the EVs arrive in a charging station in the home, a random SOC parameter (between 0 and 1) is assumed to represent the remaining storage in the EV battery.

4. Case studies and results analysis

In the case studies, a typical summer week was selected to validate the developed coordinated controls. The weather data of Ludvika was used for modelling the local renewable generations. This section first presents the individual building's electricity demand and renewable generation information. Then, the detailed EV charging and battery charging results obtained from the two scenarios (see Step 4 in Section 2) and the developed control are compared and analyzed. Finally, the overall economic and energy performances are compared.

Table 3 summarizes the input parameters used in the case studies. According to the building dimension, 100 m², 200 m² and 300 m² roof areas are planned for installing PV panels in the three buildings, respectively. It was assumed each building is installed with an electrical battery with capacity of 20 kW·h and maximum charging/ discharging rates of 6 kW. The price of purchasing electricity from the power grid was set as 0.16 € /(kW·h). Considering the negative impacts on the grid stability and safety, the feed-in-tariff was set as 0.05 € /(kW·h), which is lower than price of electricity purchase (Huang, Lovati et al. 2019). The price of electricity trading in the building cluster was set as 0.1 € /(kW·h). Such price setting will provide incentives for energy sharing within the building cluster, i.e. the building owners can earn more by selling their excessive renewable energy to the building cluster than sell to the power grid, and vice versa.

Table 3 System configuration and electricity prices

Input parameter	Value
Area of PV panel in Building A (m²)	100
Area of PV panel in Building B (m²)	200
Area of PV panel in Building C (m2)	300
Battery capacity (kW·h)	20
Battery maximum charging/discharging rates (kW)	6
Price of electricity sold to the grid (€ /(kW·h))	0.05
Price of grid electricity purchased (€ /(kW·h))	0.16
Price of electricity trading in building cluster (€)	0.1

4.1 Electricity demand, supply and mismatch

Fig. 3 displays the hourly electricity demand, hourly PV generation, and the hourly electricity mismatch of the three buildings in the selected week. Note that the heating needs of the three buildings are assumed to be met by the district heating system. Thus, the electricity demand only includes the domestic electricity loads (i.e. lighting, washing machine, TV, etc.). The trends of PV power production of the three buildings are similar, since the solar irradiation is nearly the same for the three buildings which are located in the same location. As Building C has the largest roof area, more PV panels can be installed on its roof. Thus, it has the largest average PV production.

Power mismatch of each building is calculated as the deviation between its hourly power demand and the hourly renewable generation. The diversity between the power mismatch provides good opportunities for the buildings to collaborative with each other in aspects of energy sharing. For instance, at noon (i.e. 11:00~16:00) in the first day of the selected summer week, Building A has insufficient renewable generations (i.e. 7.6 kW·h more demand), while Buildings B and C have excessive renewable generations (i.e. 24.7 kW·h and 55.8 kW·h more supply, respectively). Buildings B and C can share their surplus renewable generation with Building A to avoid grid power imports (for Building A) and power exports to the grid (for Buildings B and C), and thus help improve the overall performance at the building-cluster-level.
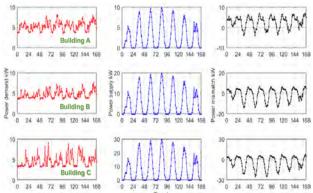

Figure 3 The hourly power demand (red), renewable generation (blue) and power mismatch (black) of the three buildings in the selected summer week

4.2 Detailed battery control and energy flow

To have a close look at the charging of EVs and battery storage, as well as the energy flow in the system, the detailed operation in the first day of the selected week is presented and analyzed in this section. Note that the EV charging loads are exactly the same for the three scenarios. The initial SOCs when EVs arrive at the charging stations are the same for three scenarios. The initial SOCs upon arrival for the three EVs are 0.29, 0.61 and 0.62, respectively. All the EVs are required to be fully charged when they depart the charging stations, i.e. SOC

equals 1. Fig. 4 presents the State of Charge (SOC) of the three EVs' battery and the aggregated battery in the first day of the selected week. For Scenarios 1 and 2, since the EVs are charged at their maximum charging rates (i.e. 4 kW, 5 kW and 10 kW for the three EVs, respectively) immediately after being plugged into the charging ports, there is a stable increase in the SOCs for all the three EVs in the beginning of parking periods. In the developed control, the EVs are charged flexibly in the parking period. In some timeslots, they are charged at a high rate; while in some timeslots, they are charged at a low rate (or even zero). Despite the different charging patterns, all the EV batteries are fully charged (as specified in the case study, see Section 3.3) before they depart the charging ports in the three scenarios.
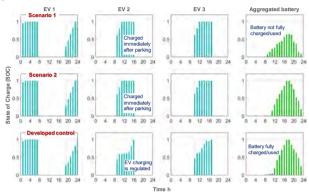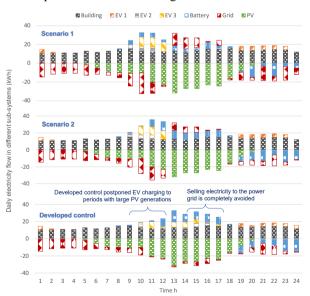

Figure 4 State of Charge (SOC) of the three EVs and the aggregated battery in the first day of selected week

Regarding the battery storage usage, the aggregated battery has not been fully charged (and thus not fully utilized) in Scenario 1, while it has been fully charged (and thus fully utilized) in Scenario 2 and the developed control. This is because in Scenario 1 the collaboration (i.e. renewable energy sharing) is not allowed among the buildings, while in Scenario 2 and the developed control, collaboration is enabled (see Fig. 6 for detailed energy sharing). The collaboration enables buildings to store their surplus renewables in other building's battery, thereby helping to increase the overall battery utilization. Such increased battery utilization can help the building cluster keep more renewable energy onsite instead of exporting to the power grid, and thus contribute to increased renewable energy self-consumption rates.

Fig. 5 depicts the electricity energy flow of the building cluster (i.e. electricity demand), aggregated PV production, power grid, aggregated battery and three EVs in the first day of the selected week for the three different scenarios. The aggregated energy exchanges within the building cluster become zero in the aggregated level, since the amount of purchased electricity from the building cluster compensates with the amount of electricity sold to the building cluster. In the period 9:00~12:00, for Scenario 1 and Scenario 2, large electricity demand occurs, as EV 2 and EV 3 are charged immediately after being plugged in. Unfortunately, the renewable energy generation is not sufficient in this

period to meet the large demands. As a result, a large amount of grid electricity is purchased by the building cluster, i.e. 48.7 kW·h and 52 kW·h for Scenarios 1 and 2, respectively. In Scenario 3 (developed control), as EV 2 and EV 3 can be flexibly charged in any timeslot during the parking period, the controllers set relatively small EV charging rates in this period. Consequently, the amount of grid power purchase is significantly reduced in the developed control, i.e. 14.6 kW·h. In the period 14:00~17:00, for Scenario 1, since there is no collaboration among buildings, only a small part of the surplus renewable energy is kept onsite, while a large part of the surplus renewables (i.e. 28.5 kW·h) is exported to the power grid at a low price. In Scenario 2, contributed by the energy sharing within building cluster, more renewable energy can be stored in the battery. After the batteries in the building cluster all being fully charged, only a small amount of surplus renewable energy (i.e. 14.1 kW·h, which is only half of the amount of exported electricity in Scenario 1) is still exported to the power grid. Scenario 2 has better performance compared with Scenario 1. Since the batteries of EV 2 and EV 3 have already been fully charged in the period 9:00~12:00, there is no energy flow for them in the period 14:00~17:00. In the developed control, considering the large renewable energy production in this period, the controller shifts the charging load of EV 2 and EV 3 to this period. Part of the surplus renewable generation is stored in the building battery and part of the surplus renewables is used to supply the EV load. As a result, exporting renewable energy to the power grid is completely avoided. This can effectively improve the renewable energy self-consumption rate of the building cluster.

Figure 5 Detailed energy flow (of building, PV systems, battery and three EVs) in the building cluster in each scenario in the first day of the selected week

To sum up, in Scenario 1, the building cluster exported 41.3 kW·h electricity to the grid and imported 177.0 kW·h electricity from the grid. In Scenario 2, the building

cluster exported 23.0 kW·h electricity to the grid and imported 159 kW·h electricity from the grid. Scenario 2 performs better than Scenario 1 (i.e. with reduced energy imports/exports) as energy sharing enables the building cluster to keep more renewable energy on-site. While using the developed control, the building cluster exported 0 kW·h electricity to the grid and imported 135.6 kW·h electricity from the grid. Scenario 3 performs even better than Scenario 2 (i.e. with reduced energy imports/exports), as the controller shifts EV charging loads to periods with large renewable production (and thus help keep more renewable energy used onsite in case the batteries have been fully charged).

4.3 Economic and energy performance comparison

This section compares the overall economic and energy performance of different controls. Table 4 summarizes the building-cluster-level daily electricity costs and renewable energy self-consumption rates. in different scenarios. Fig. 6(a) compares the daily renewable energy self-consumption rates of the three scenarios in the selected week. The relative performances improvements of Scenario 2 and the developed control compared with Scenario 1 are also depicted. Compared with Scenario 1, Scenario 2 improved the renewable energy self-consumption by 5%~24%. This is because the collaboration enables buildings to share their surplus renewable energy with other buildings with insufficient supply and thus help reduce the electricity exports to the power grid (i.e. keep more renewable energy onsite). Compared with Scenario 2, the developed control further improves the renewable self-consumption rates by 2% to 12%. This is because the developed control makes use of the flexible charging ability of EVs. By shifting the EV charging load to periods with large renewable generation periods, more renewable energy can be used onsite, especially when the electrical battery storages are fully charged.
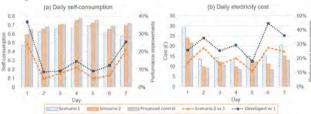

Figure 6 Comparison of the daily renewable energy self-consumption rates and electricity costs of the three scenarios

Fig. 6(b) compares the daily electricity costs of the three scenarios in the selected week. Due to increased renewable energy self-consumption rates and thus less grid power purchase, Scenario 2 achieves 11%~28% cost saving compared with Scenario 1, and the developed control achieves 7%~17% more cost saving compared with Scenario 2 (see Table 4). The relative improvements in economic performance is much larger than the relative improvements in daily self-consumption rates. This is because the building cluster purchase electricity from the

power grid at a high price (i.e. 0.16 € /(kW·h)) but sell electricity at a much lower price (i.e. 0.05 € /(kW·h)). When the building cluster exports more renewables to the power grid (i.e. in Scenario 1), they will need to buy more electricity from the grid at a high price, as the aggregated daily electricity demand is fixed.

5. Conclusion

This study has proposed a coordinated control of building clusters for improving the cluster-level performance, with both energy sharing and EV charging considered. The developed coordinated control first uses a 'representative' building to represent the whole building cluster and optimizes its energy storage operation as well as the EV charging using genetic algorithm. The optimized performance of the building cluster is considered to be the optimal one that maximizes the energy sharing within the building cluster by coordinating individual building's operation. Then, non-linear programming is used to coordinate the operation of each individual building. For validation, the developed control has been tested using the energy demand and supply data on a real buildings cluster (with three EVs considered) in Ludvika, Sweden, and its detailed energy performance (i.e. renewable self-consumption rate) and economic performance (i.e. electricity cost) have been compared with two scenarios (i.e. one does not enable energy sharing and one allows full energy sharing, both do not have EV charging controls). The major findings are summarized as follows:

- The developed coordinated control provides a mechanism to coordinate each single building's operation and EV charging demands for improved building cluster performances.

- In aspect of renewable utilization, the coordinated control improved the daily self-consumption rates by as much as 37% compared with Scenario 1 and as much as 12% compared with Scenario 2. This is because the developed control shifts the EV charging load to periods with large renewable generation periods, and thus more renewable energy are used onsite, especially when the electrical battery storages are fully charged. Note that the time of departure is an important factor affecting the EV charging control and is considered as a known input in this study decided by the EV owner. In return, EV owner can be charged less for the electricity usage.

- In aspect of economic costs, the coordinated control reduced the daily electricity costs by as much as 36% compared with Scenario and as much as 17% compared with Scenario 2. This is because the developed control reduces the amount of high-price grid electricity imports.

In this study, the detailed driving patterns of EVs are not considered, and the SOC when they arrive the charging ports are determined by some random values. Future work will take account of the predictive EV driving patterns in the optimization to achieve better performances.

Meanwhile, the uncertainty in demand and renewable prediction is not considered in this study. Future work will try to develop more robust controls.

Acknowledgments

References

Barone, G., A. Buonomano, F. Calise, C. Forzano and A. Palombo (2019). "Building to vehicle to building concept toward a novel zero energy paradigm: Modelling and case studies." Renewable and Sustainable Energy Reviews **101**: 625-648.

Dallinger, D., S. Gerda and M. Wietschel (2013). "Integration of intermittent renewable power supply using grid-connected vehicles – A 2030 case study for California and Germany." Applied Energy **104**: 666-682.

Fan, C., G. Huang and Y. Sun (2018). "A collaborative control optimization of grid-connected net zero energy buildings for performance improvements at building group level." Energy **164**: 536-549.

Gao, D.-c. and Y. Sun (2016). "A GA-based coordinated demand response control for building group level peak demand limiting with benefits to grid power balance." Energy and Buildings **110**: 31-40.

Geth, F., K. Willekens, K. Clement, J. Driesen and S. D. Breucker (2010). Impact-analysis of the charging of plug-in hybrid vehicles on the production park in Belgium. Melecon 2010 - 2010 15th IEEE Mediterranean Electrotechnical Conference.

Huang, P., B. Copertaro, X. Zhang, J. Shen, I. Löfgren, M. Rönnelid, J. Fahlen, D. Andersson and M. Svanfeldt (2020). "A review of data centers as prosumers in district energy systems: Renewable energy integration and waste heat reuse for district heating." Applied Energy **258**: 114109.

Huang, P., M. Lovati, X. Zhang, C. Bales, S. Hallbeck, A. Becker, H. Bergqvist, J. Hedberg and L. Maturi (2019). "Transforming a residential building cluster into electricity prosumers in Sweden: Optimal design of a coupled PV-heat pump-thermal storage-electric vehicle system." Applied Energy **255**: 113864.

Huang, P., H. Wu, G. Huang and Y. Sun (2018). "A top-down control method of nZEBs for performance optimization at nZEB-cluster-level." Energy **159**: 891-904.

Klein, S., W. Beckman, J. Mitchell, J. Duffie, N. Duffie, T. Freeman, J. Mitchell, J. Braun, B. Evans and J. Kummer (2004). "TRNSYS 16–A TRaNsient system simulation program, user manual." Solar Energy Laboratory. Madison: University of Wisconsin-Madison.

Lu, Y., S. Wang, Y. Sun and C. Yan (2015). "Optimal scheduling of buildings with energy generation and thermal energy storage under dynamic electricity pricing using mixed-integer nonlinear programming." Applied Energy **147**: 49-58.

Luthander, R., J. Widén, J. Munkhammar and D. Lingfors (2016). "Self-consumption enhancement and peak shaving of residential photovoltaics using storage and curtailment." Energy **112**: 221-231.

Odonkor, P. and K. Lewis (2015). Adaptive Operation Decisions in Net Zero Building Clusters.

Prasad, A. and I. Dusparic (2019). Multi-agent Deep Reinforcement Learning for Zero Energy Communities.

Salom, J., J. Widén, J. Candanedo, I. Sartori, K. Voss and A. Marszal (2011). Understanding net zero energy buildings: evaluation of load matching and grid interaction indicators. proceedings of building simulation.

Shen, L., Z. Li and Y. Sun (2016). "Performance evaluation of conventional demand response at building-group-level under different electricity pricings." Energy and Buildings **128**: 143-154.

Sun, Y., G. Huang, X. Xu and A. C.-K. Lai (2018). "Building-group-level performance evaluations of net zero energy buildings with non-collaborative controls." Applied Energy **212**: 565-576.

Taşçıkaraoğlu, A. (2018). "Economic and operational benefits of energy storage sharing for a neighborhood of prosumers in a dynamic pricing environment." Sustainable Cities and Society **38**: 219-229.

Usman, M., L. Knapen, A.-U.-H. Yasar, Y. Vanrompay, T. Bellemans, D. Janssens and G. Wets (2016). "A coordinated Framework for Optimized Charging of EV Fleet in Smart Grid." Procedia Computer Science **94**: 332-339.

Ustun, T. S., A. Zayegh and C. Ozansoy (2013). "Electric Vehicle Potential in Australia Its Impact on Smart Grids." Industrial Electronics Magazine, IEEE **7**: 15-25.

Zhao, Y., Y. Lu, C. Yan and S. Wang (2015). "MPC-based optimal scheduling of grid-connected low energy buildings with thermal energy storages." Energy and Buildings **86**: 415-426.